Acta Cryst E
CRYSTALLOGRAPHIC COMMUNICATIONS
ISSN 2056-9890

Crystal structure of {N^1,N^3-bis[(1-*tert*-butyl-1*H*-1,2,3-triazol-4-yl)methylidene]-2,2-dimethylpropane-1,3-diamine}bis(thiocyanato)iron(II)

Kateryna Znovjyak,[a] Maksym Seredyuk,[a]* Sergey O. Malinkin,[a] Iryna O. Golenya,[a] Vladimir M. Amirkhanov,[a] Sergiu Shova[b] and Nurullo U. Mulloev[c]*

[a]Department of Chemistry, Taras Shevchenko National University of Kyiv, Volodymyrska Street 64, Kyiv, 01601, Ukraine, [b]Department of Inorganic Polymers, "Petru Poni" Institute of Macromolecular, Chemistry, Romanian Academy of Science, Aleea Grigore Ghica Voda 41-A, Iasi, 700487, Romania, and [c]The Faculty of Physics, Tajik National University, Rudaki Avenue 17, Dushanbe, 734025, Tajikistan. *Correspondence e-mail: mlseredyuk@gmail.com, voruch@eml.ru

Received 19 April 2021
Accepted 24 April 2021

Edited by G. Diaz de Delgado, Universidad de Los Andes, Venezuela

Keywords: iron(II) complex; thiocyanate complex; high-spin state; trigonal distortion; magnetism; energy frameworks; crystal structure.

CCDC reference: 2079827

Supporting information: this article has supporting information at journals.iucr.org/e

The unit cell of the title compound, [$Fe^{II}(NCS)_2(C_{19}H_{32}N_8)$], consists of two charge-neutral complex molecules. In the complex molecule, the tetradentate ligand N^1,N^3-bis[(1-*tert*-butyl-1*H*-1,2,3-triazol-4-yl)methylene]-2,2-dimethylpropane-1,3-diamine coordinates to the Fe^{II} ion through the N atoms of the 1,2,3-triazole and aldimine groups. Two thiocyanate anions, also coordinated through their N atoms, complete the coordination sphere of the central Fe ion. In the crystal, neighbouring molecules are linked through weak C—H···C/S/N interactions into a three-dimensional network. The intermolecular contacts were quantified using Hirshfeld surface analysis and two-dimensional fingerprint plots, revealing the relative contributions of the contacts to the crystal packing to be H···H 50.8%, H···C/C···H 14.3%, H···S/S···H 20.5% and H···N/N···H 12.1%. The average Fe—N bond distance is 2.170 Å, indicating the high-spin state of the Fe^{II} ion, which does not change upon cooling, as demonstrated by low-temperature magnetic susceptibility measurements. DFT calculations of energy frameworks at the B3LYP/6–31 G(d,p) theory level were performed to account for the interactions involved in the crystal structure.

1. Chemical context

An interesting class of coordination compounds exhibiting spin-state switching between low- and high-spin states is represented by Fe^{II} complexes based on Schiff bases derived from N-substituted 1,2,3-triazole aldehydes (Hagiwara *et al.*, 2014, 2016, 2020; Hora & Hagiwara, 2017). In all of the charge-neutral mononuclear complexes of this kind described so far, the thiocyanate anions occupy the axial position in the coordination sphere and thus are in a *trans*-configuration (Hagiwara & Okada, 2016; Hagiwara *et al.*, 2017).

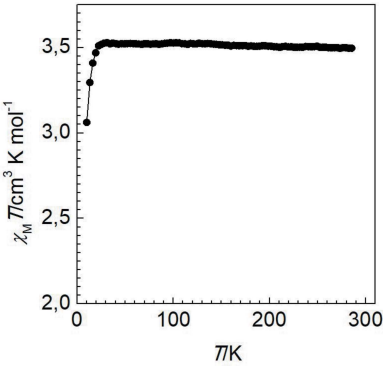

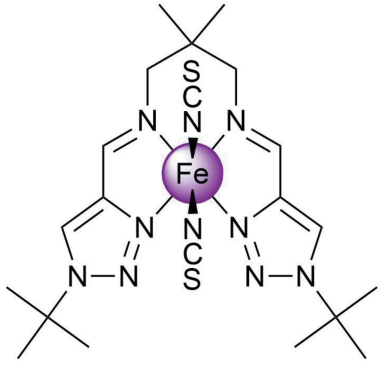

Having interest in functional 3*d* metal complexes formed by polydentate ligands (Seredyuk *et al.*, 2006, 2007, 2011, 2012, 2015, 2016; Valverde-Muñoz *et al.*, 2020), we report here a continuation of our ongoing exploration of new Fe^{II} *cis*-complexes with thiocyanate anions and tetradentate ligands N^1,N^3-bis[(1-*R*-1*H*-1,2,3-triazol-4-yl)methylene]-2,2-dimethylpropane-1,3-diamine, and report below structural and magnetic investigations of a new complex with *R* = *tert*-butyl.

2. Structural commentary

The Fe^{II} ion of the title complex has a distorted trigonal–prismatic N_6 coordination environment formed by the four N atoms of the tetradentate Schiff-base ligand and the two NCS^- counter-ions (Fig. 1). The average bond length, <Fe—N> = 2.170 (4) Å, is typical for high-spin complexes with an $[FeN_6]$ chromophore (Gütlich & Goodwin, 2004). The N—Fe—N′ angle between the *cis*-aligned thiocyanate N atoms is 91.91 (8)°. The average trigonal distortion parameters, $\Sigma = \Sigma_1^{12}(|90 - \varphi_i|)$, where φ_i is the angle N—Fe—N′ (Drew *et al.*, 1995), $\Theta = \Sigma_1^{24}(|60 - \theta_i|)$, where θ_i is the angle generated by superposition of two opposite faces of an octahedron (Chang *et al.*, 1990) are 127.8 and 438.2°, respectively. The values reveal a great deviation of the coordination environment from an ideal octahedron (where $\Sigma = \Theta = 0$), and are significantly larger than those of similar $[FeN_6]$ high-spin *trans*-complexes (Hagiwara *et al.*, 2017). With the aid of continuous shape measurements (CShM), the closest shape of a coordination polyhedron and its distortion can be determined numerically (Kershaw Cook *et al.*, 2015). The calculated CShM value relative to ideal O_h symmetry is 3.829, while it is 6.709 relative to the ideal D_{3h} trigonal–prismatic symmetry. Hence, the polyhedron is closer to the former geometry, but is still appreciably distorted, as indicated by the calculated value (for an ideal polyhedron CShM = 0). The volume of the $[FeN_6]$ coordination polyhedron is 12.60 $Å^3$.

Table 1
Hydrogen-bond geometry (Å, °).

D—H···*A*	*D*—H	H···*A*	*D*···*A*	*D*—H···*A*
C4—H4*B*···C21^{i}	0.97	2.84	3.786 (4)	166
C5—H5···S1^{ii}	0.93	2.99	3.718 (4)	137
C7—H7···S1^{i}	0.93	2.90	3.764 (4)	155
C13—H13···S1^{iii}	0.93	2.99	3.724 (4)	137
C13—H13···C20^{iii}	0.93	2.75	3.558 (4)	146
C15—H15···S1^{iii}	0.93	2.84	3.573 (4)	137
C17—H17*A*···S2^{iv}	0.96	2.94	3.873 (4)	166
C17—H17*B*···S2^{v}	0.96	2.94	3.850 (4)	158

Symmetry codes: (i) $-x+1, -y+2, -z+1$; (ii) $x+1, y, z$; (iii) $-x, -y+1, -z+1$; (iv) $x, y-1, z$; (v) $-x, -y+1, -z$.

3. Supramolecular features

In the lattice, neighbouring complex molecules form a three-dimensional supramolecular network (Fig. 2) through the weak C—H···*X* hydrogen bonds (Table 1). No strong hydrogen bonding or stacking interactions are observed between the complex molecules in the crystal lattice.

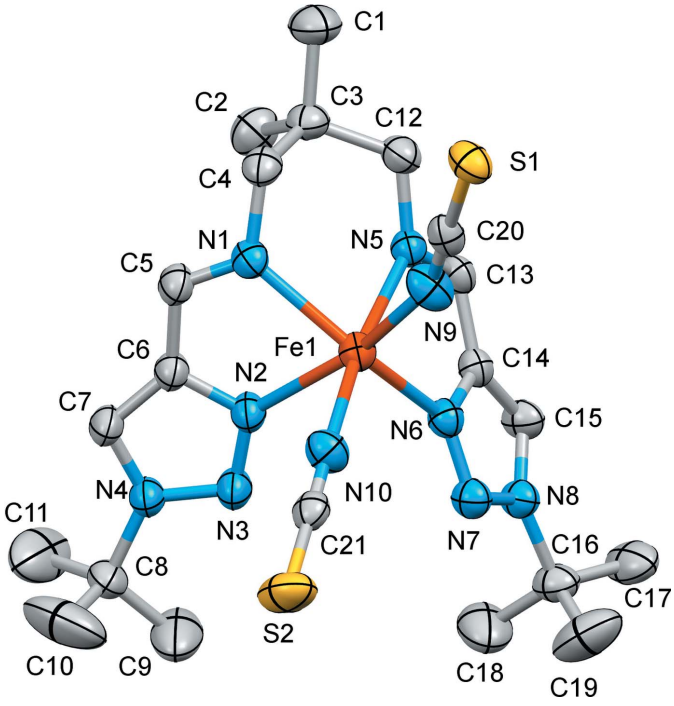

Figure 1
The molecular structure of the title compound with displacement ellipsoids drawn at the 50% probability level. H atoms have been omitted for clarity.

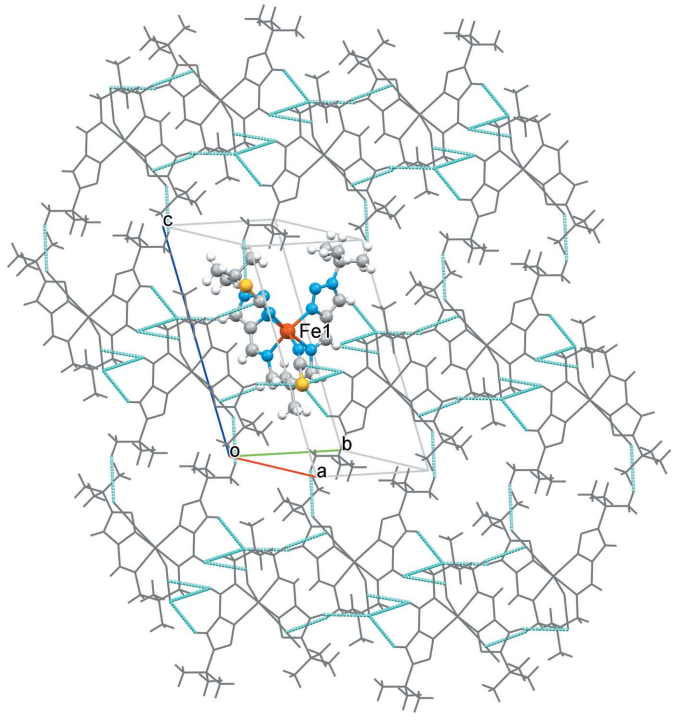

Figure 2
The packing of molecules into the three-dimensional network held together by weak C—H···C/S bonding (dashed cyan lines).

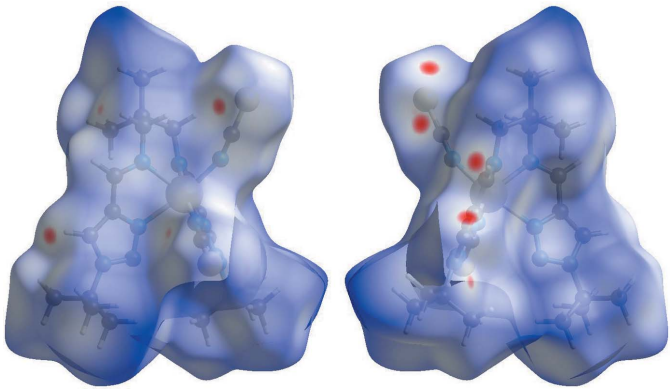

Figure 3
Two projections of d_{norm} mapped on Hirshfeld surfaces, showing the intermolecular interactions within the molecule. Red areas represent regions where contacts are shorter than the sum of the van der Waals radii, blue areas represent regions where contacts are larger than the sum of van der Waals radii, and white areas are regions where contacts are close to the sum of van der Waals radii.

4. Hirshfeld surface and 2D fingerprint plots

Hirshfeld surface analysis was performed and the associated two-dimensional fingerprint plots were generated using *Crystal Explorer* (Turner *et al.*, 2017), with a standard resolution of the three-dimensional d_{norm} surfaces plotted over a fixed colour scale of −0.1141 (red) to 1.9978 (blue) a.u. The pale-red spots symbolize short contacts and negative d_{norm} values on the surface correspond to the interactions described above. The overall two-dimensional fingerprint plot is illustrated in Fig. 3. The Hirshfeld surfaces mapped over d_{norm} are shown for the H···H, H···C/C···H, H···S/S···H, and H···N/N···H contacts, and the two-dimensional fingerprint plots are presented in Fig. 4, associated with their relative contributions to the Hirshfeld surface. At 50.8%, the largest contribution to the overall crystal packing is from H···H interactions, which are located in the middle region of the fingerprint plot. H···C/C···H contacts contribute 14.3%, and the H···S/S···H contacts contribute 20.5% to the Hirshfeld surface, both resulting in a pair of characteristic wings. The H···N/N···H contacts, represented by a pair of sharp spikes in the fingerprint plot, make a 12.1% contribution to the Hirshfeld surface.

5. Energy frameworks

The energy frameworks, calculated using the wave function at the B3LYP/6-3G(d,p) level of theory for the title compound, including the electrostatic potential forces (E_{ele}), the dispersion forces (E_{dis}) and the total energy diagrams (E_{tot}), are shown in Fig. 5*a*. The cylindrical radii, adjusted to the same scale factor of 80, are proportional to the relative strength of the corresponding energies (Turner *et al.*, 2017; Tan *et al.*, 2019). It can be seen that the major contribution to the intermolecular interactions is from Coulomb forces (E_{ele}), reflecting dipole–dipole interactions of the asymmetric complex *cis*-molecules in the lattice. According to the calculations, the most repulsive interaction is due to the anion-to-

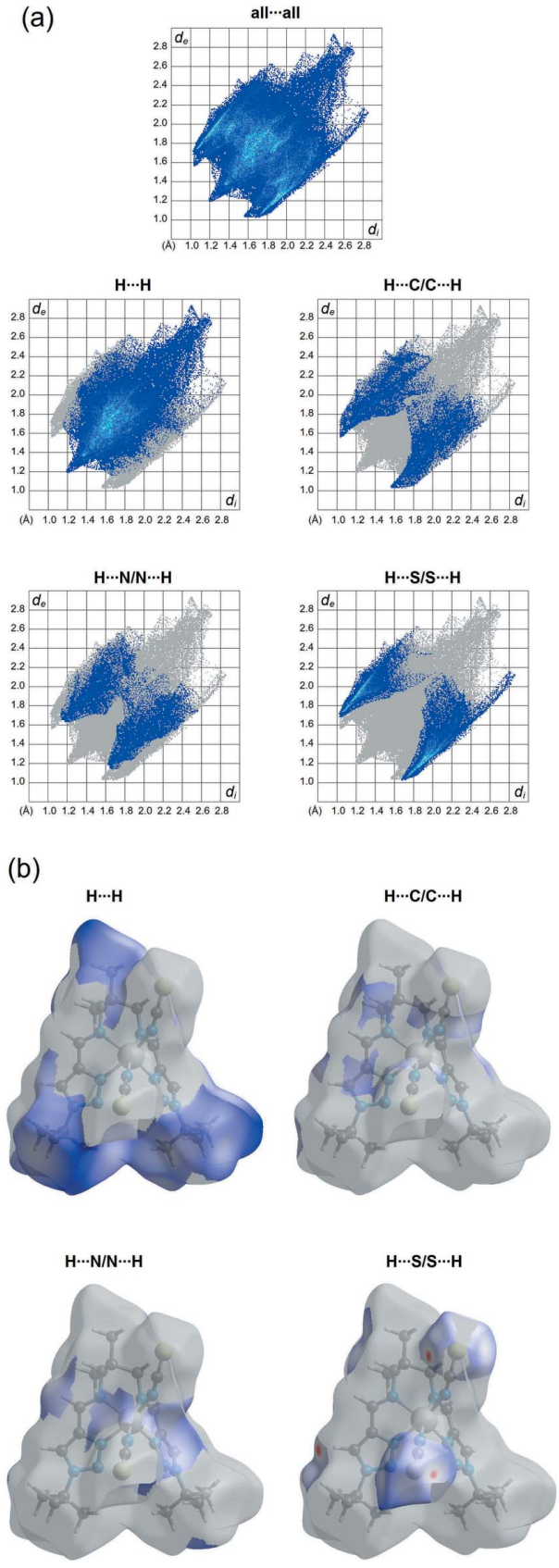

Figure 4
(*a*) The overall two-dimensional fingerprint plot and those decomposed into specified interactions. (*b*) Hirshfeld surface representations with the function d_{norm} plotted onto the surface for the different interactions.

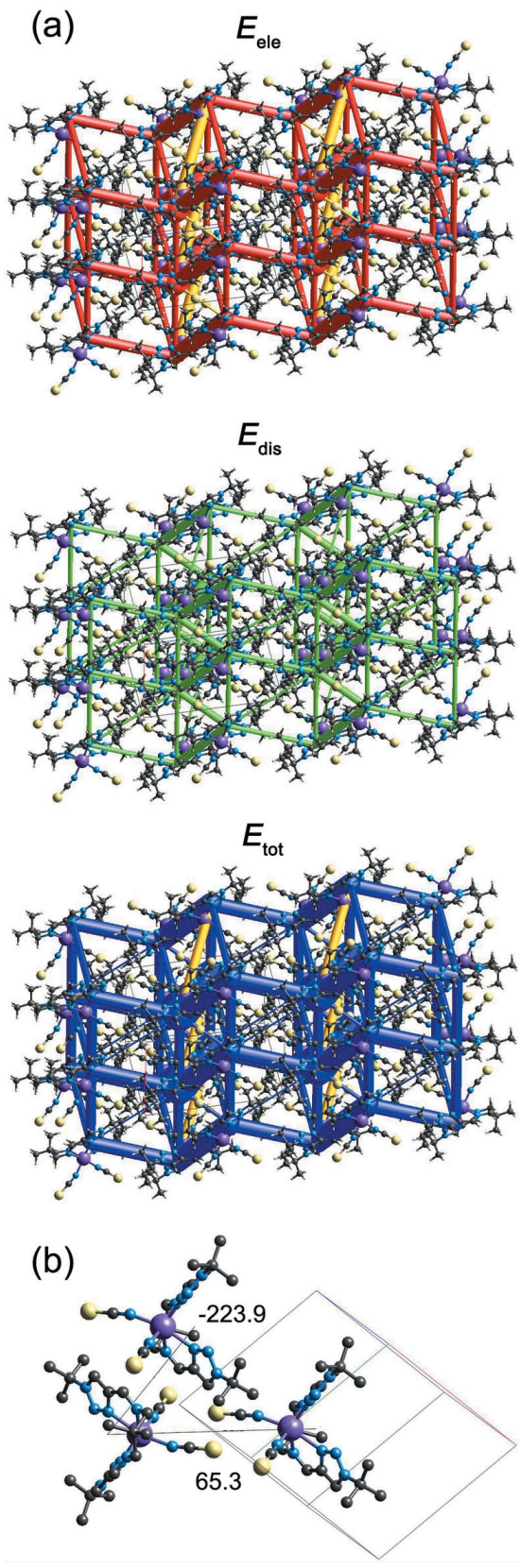

Figure 5
(*a*) The calculated energy frameworks, showing the electrostatic potential forces (E_{ele}), the dispersion forces (E_{dis}) and the total energy diagrams (E_{tot}). Yellow coloured tubes correspond to the repulsive interactions; (*b*) the strongest repulsive and attractive interactions between neighbouring complex molecules.

Table 2
Comparison of the distortion parameters (Å, °) for the indicated Fe^{II} complexes.

	<Fe—N>	Σ	Θ	CShM (O_h)	CShM (D_{3h})
Title compound	2.170	127.8	438.2	3.829	6.709
IQEFAO	2.167	127.40	481.9	4.269	5.671
CUWQAP	2.186	149.38	453.2	6.285	4.008
CABLOH	1.899	178.16	725.74	12.735	0.525
BUNSAF	2.218	201.07	703.65	13.084	1.887
OWIHAE	2.202	206.57	894.48	16.909	0.602
OTANOO[a]	2.191	183.24	697.3	12.065	1.098

Note: (*a*) Parameters averaged over five independent complex cations.

anion alignment of neighbouring complex molecules (E_{tot} = 65.3 kJ mol^{-1}) while the ligand-to-anion alignment gives the most attractive one (E_{tot} = −223.9 kJ mol^{-1}) (Fig. 5*b*). The colour-coded interaction mappings within a radius of 3.8 Å of a central reference molecule for the title compound together with full details of the various contributions to the total energy (E_{tot}) are given in the Supporting Information.

6. Magnetic properties

Variable-temperature magnetic susceptibility measurements were performed on single crystals (10 mg) of the title compound using a Quantum Design MPMS2 superconducting quantum interference device (SQUID) susceptometer operating at 1 T. Experimental susceptibilities were corrected for the diamagnetism of the holder (gelatine capsule) and of the constituent atoms by the application of Pascal's constants. The magnetic behaviour of the compound is shown in Fig. 6 in the form of $\chi_M T$ versus T (χ_M is the molar magnetic susceptibility and T is the temperature). At 300 K, the $\chi_M T$ value is close to 3.51 cm^3 K mol^{-1}, and on cooling the value remains constant

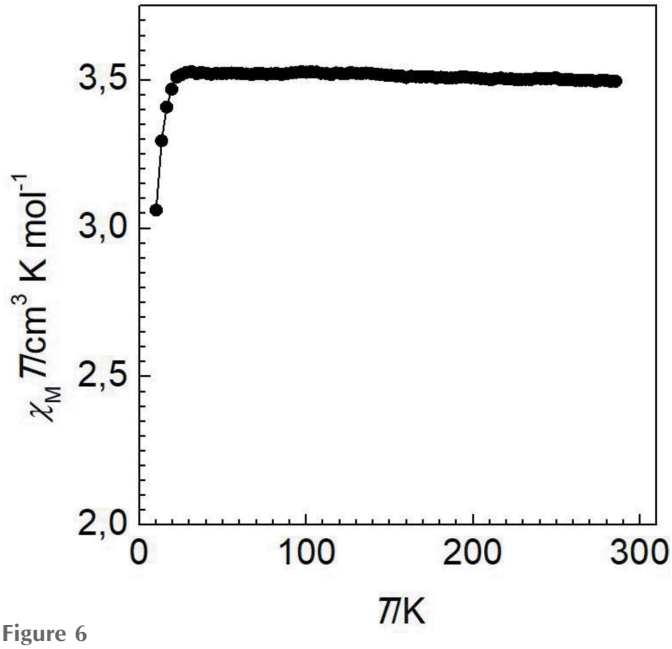

Figure 6
$\chi_M T$ *versus* T plot for the title compound.

Table 3
Experimental details.

Crystal data	
Chemical formula	$[Fe(NCS)_2(C_{19}H_{32}N_8)]$
M_r	544.53
Crystal system, space group	Triclinic, $P\overline{1}$
Temperature (K)	250
a, b, c (Å)	9.4768 (5), 10.8151 (5), 15.2493 (7)
α, β, γ (°)	102.267 (4), 102.813 (4), 103.291 (4)
V (Å^3)	1424.90 (13)
Z	2
Radiation type	Mo $K\alpha$
μ (mm^{-1})	0.70
Crystal size (mm)	0.4 × 0.2 × 0.2
Data collection	
Diffractometer	Rigaku Oxford Diffraction Xcalibur, Eos
Absorption correction	Multi-scan (*CrysAlis PRO*; Rigaku OD, 2015)
T_{min}, T_{max}	0.865, 1.000
No. of measured, independent and observed [$I > 2\sigma(I)$] reflections	10732, 5016, 4188
R_{int}	0.025
$(\sin \theta/\lambda)_{max}$ (Å^{-1})	0.595
Refinement	
$R[F^2 > 2\sigma(F^2)]$, $wR(F^2)$, S	0.038, 0.095, 1.04
No. of reflections	5016
No. of parameters	315
H-atom treatment	H-atom parameters constrained
$\Delta\rho_{max}$, $\Delta\rho_{min}$ (e Å^{-3})	0.46, −0.40

Computer programs: *CrysAlis PRO* (Rigaku OD, 2015), *SHELXT* (Sheldrick, 2015*a*), *SHELXL2018/3* (Sheldrick, 2015*b*) and *OLEX2* (Dolomanov *et al.*, 2009).

down to 30 K. The decrease of $\chi_M T$ below 30 K is attributed to the zero-field splitting of the high-spin (S = 2) Fe^{II} centres (Kahn, 1993), which corroborates with the observed long average Fe—N bond length and the large geometric distortion of the coordination polyhedron of the central Fe^{II} ion.

7. Database survey

A search of the Cambridge Structural Database (CSD, Version 5.42, last update February 2021; Groom *et al.*, 2016) reveals five similar Fe^{II} thiocyanate complexes, derivatives of a 1,3-diamine and *N*-substituted 1,2,3-triazole aldehydes: DURXEV, ADAQUU, ADAREF and solvatomorphs ADAROP and ADARUV (Hagiwara *et al.*, 2017, Hagiwara & Okada, 2016). These complexes show hysteretic spin crossover with variation of the Fe—N distances in the range 1.931–1.959 Å for the low-spin state and 2.154–2.169 Å for the high-spin state of the Fe^{II} ions. The reported pseudo-trigonal–prismatic complexes with an $[FeN_6]$ chromophore are formed by structurally hindered rigid hexadentate ligands favouring trigonal geometry of the central Fe^{II} ion: CABLOH (Voloshin *et al.*, 2001), BUNSAF (El Hajj *et al.*, 2009), OWIHAE (Seredyuk *et al.*, 2011), OTANOO (Stock *et al.*, 2016). The recently reported by us *cis*-complexes CUWQAP and IQEFAO have similar strongly distorted coordination environment of the central Fe^{II} ion (Znovjyak *et al.*, 2020, 2021). Table 2 collates the distortion parameters Σ, Θ and CShM for the pseudo-trigonal-prismatic complexes mentioned above.

8. Synthesis and crystallization

The synthesis of the title compound is identical to that reported by us recently for similar thiocyanate complexes (Znovjyak *et al.*, 2020, 2021). The ligand of the title compound was obtained *in situ* by condensation of 2,2-dimethyl-1,3-propanediamine (24 µL, 0.20 mmol) with 1-*tert*-butyl-1*H*-1,2,3-triazole-4-carbaldehyde (63 mg, 0.45 mmol) in boiling methanol (5 ml) over 5 min and subsequently reacted with $[Fe(py)_4(NCS)_2]$ (100 mg, 0.20 mmol) and ascorbic acid (11 mg, 0.06 mmol) in boiling methanol (5 ml). The formed yellow solution was slowly cooled to ambient temperature. Yellow–orange crystals then precipitated and were subsequently filtered off. Elemental analysis calculated (%) for $C_{21}H_{32}FeN_{10}S_2$: C, 46.32; H, 5.92; N, 25.72; S, 11.78. Found: C, 46.40; H, 6.10; N, 26.18; S, 11.80. IR ν (cm^{-1}, KBr): 1611 (C=N), 2071, 2116 (NCS).

9. Refinement

Crystal data, data collection and structure refinement details are summarized in Table 3. H atoms were positioned geometrically (C—H = 0.93–0.97 Å) and refined as riding with $U_{iso}(H) = 1.2U_{eq}(C)$ or $1.5U_{eq}$(C-methyl).

Acknowledgements

Author contributions are as follows: Conceptualization, NUM and MS; methodology, KZ; formal analysis, NUM; synthesis, SOM; magnetic measurements, IAG; single-crystal measurements, SS; writing (original draft), NUM and MS; writing (review and editing of the manuscript), NUM, MS, KZ, SOM, IOG, TYS and SS; visualization and DFT calculations, VMA; funding acquisition, KZ.

References

Chang, H. R., McCusker, J. K., Toftlund, H., Wilson, S. R., Trautwein, A. X., Winkler, H. & Hendrickson, D. N. (1990). *J. Am. Chem. Soc.* **112**, 6814–6827.
Dolomanov, O. V., Bourhis, L. J., Gildea, R. J., Howard, J. A. K. & Puschmann, H. (2009). *J. Appl. Cryst.* **42**, 339–341.
Drew, M. G. B., Harding, C. J., McKee, V., Morgan, G. G. & Nelson, J. (1995). *J. Chem. Soc. Chem. Commun.* pp. 1035–1038.
El Hajj, F., Sebki, G., Patinec, V., Marchivie, M., Triki, S., Handel, H., Yefsah, S., Tripier, R., Gómez-García, C. J. & Coronado, E. (2009). *Inorg. Chem.* **48**, 10416–10423.
Groom, C. R., Bruno, I. J., Lightfoot, M. P. & Ward, S. C. (2016). *Acta Cryst.* B**72**, 171–179.
Gütlich, P. & Goodwin, H. A. (2004). *Top. Curr. Chem.* **233**, 1–47.
Hagiwara, H., Masuda, T., Ohno, T., Suzuki, M., Udagawa, T. & Murai, K.-I. (2017). *Cryst. Growth Des.* **17**, 6006–6019.
Hagiwara, H., Minoura, R., Okada, S. & Sunatsuki, Y. (2014). *Chem. Lett.* **43**, 950–952.
Hagiwara, H., Minoura, R., Udagawa, T., Mibu, K. & Okabayashi, J. (2020). *Inorg. Chem.* **59**, 9866–9880.
Hagiwara, H. & Okada, S. (2016). *Chem. Commun.* **52**, 815–818.
Hagiwara, H., Tanaka, T. & Hora, S. (2016). *Dalton Trans.* **45**, 17132–17140.
Hora, S. & Hagiwara, H. (2017). *Inorganics*, **5**, 49.
Kahn, O. (1993). *Molecular Magnetism*. New York: Wiley-VCH.

Kershaw Cook, L. J., Mohammed, R., Sherborne, G., Roberts, T. D., Alvarez, S. & Halcrow, M. A. (2015). *Coord. Chem. Rev.* **289–290**, 2–12.

Rigaku OD (2015). *CrysAlis PRO*. Rigaku Oxford Diffraction, Yarnton, England.

Seredyuk, M. (2012). *Inorg. Chim. Acta*, **380**, 65–71.

Seredyuk, M., Gaspar, A. B., Ksenofontov, V., Reiman, S., Galyametdinov, Y., Haase, W., Rentschler, E. & Gütlich, P. (2006). *Hyperfine Interact.* **166**, 385–390.

Seredyuk, M., Gaspar, A. B., Kusz, J. & Gütlich, P. (2011). *Z. Anorg. Allg. Chem.* **637**, 965–976.

Seredyuk, M., Haukka, M., Fritsky, I. O., Kozłowski, H., Krämer, R., Pavlenko, V. A. & Gütlich, P. (2007). *Dalton Trans.* pp. 3183–3194.

Seredyuk, M., Piñeiro-López, L., Muñoz, M. C., Martínez-Casado, F. J., Molnár, G., Rodriguez-Velamazán, J. A., Bousseksou, A. & Real, J. A. (2015). *Inorg. Chem.* **54**, 7424–7432.

Seredyuk, M., Znovjyak, K., Muñoz, M. C., Galyametdinov, Y., Fritsky, I. O. & Real, J. A. (2016). *RSC Adv.* **6**, 39627–39635.

Sheldrick, G. M. (2015*a*). *Acta Cryst.* A**71**, 3–8.

Sheldrick, G. M. (2015*b*). *Acta Cryst.* C**71**, 3–8.

Stock, P., Deck, E., Hohnstein, S., Korzekwa, J., Meyer, K., Heinemann, F. W., Breher, F. & Hörner, G. (2016). *Inorg. Chem.* **55**, 5254–5265.

Tan, S. L., Jotani, M. M. & Tiekink, E. R. T. (2019). *Acta Cryst.* E**75**, 308–318.

Turner, M. J., Mckinnon, J. J., Wolff, S. K., Grimwood, D. J., Spackman, P. R., Jayatilaka, D. & Spackman, M. A. (2017). *Crystal Explorer 17.5*. University of Western Australia.

Valverde-Muñoz, F., Seredyuk, M., Muñoz, M. C., Molnár, G., Bibik, Y. S. & Real, J. A. (2020). *Angew. Chem. Int. Ed.* **59**, 18632–18638.

Voloshin, Y. Z., Varzatskii, O. A., Stash, A. I., Belsky, V. K., Bubnov, Y. N., Vorontsov, I. I., Potekhin, K. A., Antipin, M. Y. & Polshin, E. V. (2001). *Polyhedron*, **20**, 2721–2733.

Znovjyak, K., Seredyuk, M., Malinkin, S. O., Golenya, I. A., Sliva, T. Y., Shova, S. & Mulloev, N. U. (2021). *Acta Cryst.* E**77**, 495–499.

Znovjyak, K., Seredyuk, M., Malinkin, S. O., Shova, S. & Soliev, L. (2020). *Acta Cryst.* E**76**, 1661–1664.

supporting information

Acta Cryst. (2021). E**77**, 573-578 [https://doi.org/10.1107/S2056989021004412]

Crystal structure of {N^1,N^3-bis[(1-*tert*-butyl-1*H*-1,2,3-triazol-4-yl)methylidene]-2,2-dimethylpropane-1,3-diamine}bis(thiocyanato)iron(II)

Kateryna Znovjyak, Maksym Seredyuk, Sergey O. Malinkin, Iryna O. Golenya, Vladimir M. Amirkhanov, Sergiu Shova and Nurullo U. Mulloev

Computing details

Data collection: *CrysAlis PRO* (Rigaku OD, 2015); cell refinement: *CrysAlis PRO* (Rigaku OD, 2015); data reduction: *CrysAlis PRO* (Rigaku OD, 2015); program(s) used to solve structure: ShelXT (Sheldrick, 2015a); program(s) used to refine structure: *SHELXL2018/3* (Sheldrick, 2015b); molecular graphics: *OLEX2* (Dolomanov *et al.*, 2009); software used to prepare material for publication: *OLEX2* (Dolomanov *et al.*, 2009).

{N^1,N^3-Bis[(1-*tert*-butyl-1*H*-1,2,3-triazol-4-yl)methylidene]-2,2-dimethylpropane-1,3-diamine}bis(thiocyanato)iron(II)

Crystal data

$[Fe(NCS)_2(C_{19}H_{32}N_8)]$
M_r = 544.53
Triclinic, $P\overline{1}$
a = 9.4768 (5) Å
b = 10.8151 (5) Å
c = 15.2493 (7) Å
α = 102.267 (4)°
β = 102.813 (4)°
γ = 103.291 (4)°
V = 1424.90 (13) Å^3
Z = 2
F(000) = 572
D_x = 1.269 Mg m^{-3}
Mo $K\alpha$ radiation, λ = 0.71073 Å
Cell parameters from 3729 reflections
θ = 2.0–26.8°
μ = 0.70 mm^{-1}
T = 250 K
Prism, orange
0.4 × 0.2 × 0.2 mm

Data collection

Rigaku Oxford Diffraction Xcalibur, Eos diffractometer
Detector resolution: 16.1593 pixels mm^{-1}
ω scans
Absorption correction: multi-scan (CrysAlisPro; Rigaku OD, 2015)
T_{min} = 0.865, T_{max} = 1.000
10732 measured reflections
5016 independent reflections
4188 reflections with $I > 2\sigma(I)$
R_{int} = 0.025
θ_{max} = 25.0°, θ_{min} = 2.0°
h = −10→11
k = −12→12
l = −18→18

Refinement

Refinement on F^2
Least-squares matrix: full
$R[F^2 > 2\sigma(F^2)]$ = 0.038
$wR(F^2)$ = 0.095
S = 1.04
5016 reflections
315 parameters
0 restraints
Primary atom site location: dual
Hydrogen site location: inferred from neighbouring sites
H-atom parameters constrained

$w = 1/[\sigma^2(F_o^2) + (0.0371P)^2 + 0.545P]$
where $P = (F_o^2 + 2F_c^2)/3$
$(\Delta/\sigma)_{max} = 0.001$
$\Delta\rho_{max} = 0.46$ e Å^{-3}
$\Delta\rho_{min} = -0.40$ e Å^{-3}

Special details

Geometry. All esds (except the esd in the dihedral angle between two l.s. planes) are estimated using the full covariance matrix. The cell esds are taken into account individually in the estimation of esds in distances, angles and torsion angles; correlations between esds in cell parameters are only used when they are defined by crystal symmetry. An approximate (isotropic) treatment of cell esds is used for estimating esds involving l.s. planes.

Fractional atomic coordinates and isotropic or equivalent isotropic displacement parameters (Å²)

	x	*y*	*z*	U_{iso}*/U_{eq}
Fe1	0.23066 (4)	0.71954 (3)	0.39637 (2)	0.03412 (12)
S1	−0.02770 (8)	0.91016 (6)	0.59945 (5)	0.04605 (18)
S2	0.18981 (11)	0.99900 (8)	0.18833 (5)	0.0709 (3)
N1	0.4279 (2)	0.81942 (18)	0.51741 (13)	0.0362 (5)
N2	0.4378 (2)	0.70935 (19)	0.34658 (14)	0.0382 (5)
N3	0.4618 (2)	0.6739 (2)	0.26556 (14)	0.0422 (5)
N4	0.6061 (2)	0.73984 (19)	0.27554 (14)	0.0397 (5)
N5	0.2174 (2)	0.57207 (18)	0.47997 (13)	0.0347 (4)
N6	0.1170 (2)	0.52968 (18)	0.29454 (13)	0.0359 (5)
N7	0.0625 (2)	0.48742 (19)	0.20347 (14)	0.0399 (5)
N8	0.0220 (2)	0.35431 (18)	0.18153 (13)	0.0386 (5)
N9	0.0762 (3)	0.7799 (2)	0.46068 (16)	0.0504 (6)
N10	0.2124 (2)	0.8439 (2)	0.31141 (15)	0.0466 (5)
C1	0.3934 (4)	0.7358 (3)	0.74168 (19)	0.0664 (9)
H1A	0.488965	0.795885	0.780643	0.100*
H1B	0.375591	0.655489	0.760243	0.100*
H1C	0.314239	0.775546	0.748319	0.100*
C2	0.5250 (3)	0.6455 (3)	0.6288 (2)	0.0570 (7)
H2A	0.522605	0.621296	0.564042	0.086*
H2B	0.513695	0.568366	0.651321	0.086*
H2C	0.619922	0.709544	0.664560	0.086*
C3	0.3958 (3)	0.7047 (2)	0.63914 (16)	0.0427 (6)
C4	0.4194 (3)	0.8373 (2)	0.61365 (16)	0.0405 (6)
H4A	0.336116	0.872821	0.620707	0.049*
H4B	0.512065	0.900330	0.656164	0.049*
C5	0.5577 (3)	0.8462 (2)	0.50359 (17)	0.0406 (6)
H5	0.644384	0.894529	0.552199	0.049*
C6	0.5647 (3)	0.7985 (2)	0.40914 (16)	0.0370 (6)
C7	0.6733 (3)	0.8177 (2)	0.36351 (17)	0.0430 (6)
H7	0.772226	0.872582	0.387956	0.052*
C8	0.6700 (3)	0.7264 (3)	0.19420 (18)	0.0487 (7)
C9	0.5645 (4)	0.6141 (4)	0.1149 (2)	0.1047 (15)
H9A	0.550373	0.534196	0.134109	0.157*
H9B	0.606340	0.604349	0.062876	0.157*
H9C	0.468901	0.631363	0.096737	0.157*
C10	0.6890 (6)	0.8558 (4)	0.1695 (3)	0.1240 (18)

H10A	0.592928	0.873393	0.155227	0.186*
H10B	0.727368	0.850811	0.116084	0.186*
H10C	0.758785	0.925718	0.221622	0.186*
C11	0.8222 (4)	0.7048 (5)	0.2252 (3)	0.1079 (15)
H11A	0.887477	0.779295	0.275755	0.162*
H11B	0.865439	0.695136	0.173773	0.162*
H11C	0.810879	0.626152	0.245908	0.162*
C12	0.2433 (3)	0.6048 (2)	0.58150 (16)	0.0436 (6)
H12A	0.235390	0.523925	0.600421	0.052*
H12B	0.163402	0.639851	0.596548	0.052*
C13	0.1634 (3)	0.4524 (2)	0.43216 (17)	0.0388 (6)
H13	0.155551	0.384125	0.460660	0.047*
C14	0.1140 (3)	0.4256 (2)	0.33115 (16)	0.0343 (5)
C15	0.0539 (3)	0.3127 (2)	0.25822 (17)	0.0416 (6)
H15	0.038598	0.225792	0.261304	0.050*
C16	−0.0388 (3)	0.2749 (3)	0.08089 (17)	0.0479 (7)
C17	−0.1268 (4)	0.1368 (3)	0.0764 (2)	0.0696 (9)
H17A	−0.060908	0.096972	0.110571	0.104*
H17B	−0.166885	0.084533	0.012288	0.104*
H17C	−0.208368	0.141301	0.103520	0.104*
C18	0.0941 (4)	0.2720 (4)	0.0434 (2)	0.0891 (12)
H18A	0.146877	0.360201	0.045494	0.134*
H18B	0.059447	0.217558	−0.020213	0.134*
H18C	0.161008	0.236346	0.080741	0.134*
C19	−0.1432 (5)	0.3412 (3)	0.0304 (2)	0.0919 (13)
H19A	−0.226092	0.341066	0.056965	0.138*
H19B	−0.181430	0.293743	−0.034808	0.138*
H19C	−0.088105	0.430716	0.037174	0.138*
C20	0.0333 (3)	0.8349 (2)	0.51828 (18)	0.0367 (6)
C21	0.2028 (3)	0.9064 (2)	0.25931 (17)	0.0390 (6)

Atomic displacement parameters (Å²)

	U^{11}	U^{22}	U^{33}	U^{12}	U^{13}	U^{23}
Fe1	0.0342 (2)	0.03043 (19)	0.0383 (2)	0.01036 (15)	0.01232 (16)	0.00759 (15)
S1	0.0547 (4)	0.0404 (4)	0.0486 (4)	0.0136 (3)	0.0264 (3)	0.0117 (3)
S2	0.0981 (7)	0.0621 (5)	0.0433 (4)	0.0113 (5)	0.0066 (4)	0.0230 (4)
N1	0.0387 (12)	0.0299 (10)	0.0377 (11)	0.0076 (9)	0.0129 (9)	0.0052 (9)
N2	0.0317 (11)	0.0383 (11)	0.0399 (12)	0.0052 (9)	0.0124 (9)	0.0040 (9)
N3	0.0318 (11)	0.0451 (12)	0.0424 (12)	0.0044 (9)	0.0111 (10)	0.0040 (10)
N4	0.0324 (11)	0.0432 (12)	0.0388 (12)	0.0054 (9)	0.0116 (9)	0.0059 (10)
N5	0.0328 (11)	0.0337 (11)	0.0369 (11)	0.0075 (9)	0.0115 (9)	0.0087 (9)
N6	0.0359 (11)	0.0324 (10)	0.0390 (12)	0.0085 (9)	0.0124 (9)	0.0090 (9)
N7	0.0447 (12)	0.0340 (11)	0.0402 (12)	0.0093 (9)	0.0125 (10)	0.0104 (9)
N8	0.0447 (12)	0.0324 (11)	0.0361 (11)	0.0068 (9)	0.0119 (9)	0.0082 (9)
N9	0.0538 (14)	0.0530 (14)	0.0625 (15)	0.0297 (12)	0.0297 (12)	0.0242 (12)
N10	0.0500 (14)	0.0437 (12)	0.0516 (14)	0.0159 (11)	0.0188 (11)	0.0181 (11)
C1	0.079 (2)	0.072 (2)	0.0385 (16)	0.0090 (17)	0.0176 (15)	0.0089 (15)

C2	0.0541 (18)	0.0564 (18)	0.0582 (18)	0.0216 (14)	0.0080 (15)	0.0133 (15)
C3	0.0466 (15)	0.0469 (15)	0.0328 (13)	0.0131 (12)	0.0118 (12)	0.0075 (11)
C4	0.0392 (14)	0.0411 (14)	0.0360 (13)	0.0102 (11)	0.0125 (11)	−0.0006 (11)
C5	0.0345 (14)	0.0369 (13)	0.0413 (14)	0.0027 (11)	0.0086 (11)	0.0031 (11)
C6	0.0312 (13)	0.0359 (13)	0.0377 (13)	0.0042 (10)	0.0091 (11)	0.0046 (11)
C7	0.0322 (14)	0.0458 (15)	0.0391 (14)	−0.0006 (11)	0.0081 (11)	0.0022 (12)
C8	0.0420 (15)	0.0608 (17)	0.0390 (14)	0.0065 (13)	0.0173 (12)	0.0078 (13)
C9	0.079 (3)	0.138 (4)	0.056 (2)	−0.011 (2)	0.0318 (19)	−0.025 (2)
C10	0.209 (6)	0.103 (3)	0.096 (3)	0.043 (3)	0.095 (4)	0.051 (3)
C11	0.063 (2)	0.195 (5)	0.072 (2)	0.055 (3)	0.034 (2)	0.014 (3)
C12	0.0479 (15)	0.0437 (15)	0.0394 (14)	0.0078 (12)	0.0188 (12)	0.0114 (12)
C13	0.0397 (14)	0.0334 (13)	0.0429 (14)	0.0056 (11)	0.0123 (11)	0.0147 (11)
C14	0.0328 (13)	0.0313 (12)	0.0388 (13)	0.0076 (10)	0.0121 (11)	0.0096 (10)
C15	0.0528 (16)	0.0313 (13)	0.0401 (14)	0.0090 (12)	0.0134 (12)	0.0121 (11)
C16	0.0617 (18)	0.0425 (15)	0.0342 (14)	0.0104 (13)	0.0118 (13)	0.0069 (12)
C17	0.094 (3)	0.0498 (17)	0.0418 (16)	−0.0047 (17)	0.0119 (16)	0.0000 (14)
C18	0.088 (3)	0.103 (3)	0.059 (2)	0.004 (2)	0.039 (2)	−0.006 (2)
C19	0.117 (3)	0.079 (2)	0.057 (2)	0.032 (2)	−0.017 (2)	0.0112 (18)
C20	0.0338 (13)	0.0346 (13)	0.0487 (15)	0.0130 (11)	0.0141 (12)	0.0202 (12)
C21	0.0364 (14)	0.0363 (13)	0.0354 (14)	0.0057 (11)	0.0075 (11)	−0.0003 (12)

Geometric parameters (Å, º)

Fe1—N1	2.182 (2)	C4—H4B	0.9700
Fe1—N2	2.2733 (19)	C5—H5	0.9300
Fe1—N5	2.2422 (19)	C5—C6	1.445 (3)
Fe1—N6	2.1619 (19)	C6—C7	1.367 (3)
Fe1—N9	2.082 (2)	C7—H7	0.9300
Fe1—N10	2.066 (2)	C8—C9	1.489 (4)
S1—C20	1.623 (3)	C8—C10	1.507 (4)
S2—C21	1.628 (3)	C8—C11	1.502 (4)
N1—C4	1.462 (3)	C9—H9A	0.9600
N1—C5	1.273 (3)	C9—H9B	0.9600
N2—N3	1.300 (3)	C9—H9C	0.9600
N2—C6	1.361 (3)	C10—H10A	0.9600
N3—N4	1.347 (3)	C10—H10B	0.9600
N4—C7	1.345 (3)	C10—H10C	0.9600
N4—C8	1.491 (3)	C11—H11A	0.9600
N5—C12	1.463 (3)	C11—H11B	0.9600
N5—C13	1.264 (3)	C11—H11C	0.9600
N6—N7	1.307 (3)	C12—H12A	0.9700
N6—C14	1.356 (3)	C12—H12B	0.9700
N7—N8	1.348 (3)	C13—H13	0.9300
N8—C15	1.338 (3)	C13—C14	1.451 (3)
N8—C16	1.498 (3)	C14—C15	1.370 (3)
N9—C20	1.156 (3)	C15—H15	0.9300
N10—C21	1.149 (3)	C16—C17	1.513 (4)
C1—H1A	0.9600	C16—C18	1.498 (4)

C1—H1B	0.9600	C16—C19	1.519 (4)
C1—H1C	0.9600	C17—H17A	0.9600
C1—C3	1.535 (3)	C17—H17B	0.9600
C2—H2A	0.9600	C17—H17C	0.9600
C2—H2B	0.9600	C18—H18A	0.9600
C2—H2C	0.9600	C18—H18B	0.9600
C2—C3	1.529 (4)	C18—H18C	0.9600
C3—C4	1.545 (3)	C19—H19A	0.9600
C3—C12	1.531 (3)	C19—H19B	0.9600
C4—H4A	0.9700	C19—H19C	0.9600

N1—Fe1—N2	73.16 (7)	N4—C7—H7	127.5
N1—Fe1—N5	78.59 (7)	C6—C7—H7	127.5
N5—Fe1—N2	102.76 (7)	N4—C8—C10	106.5 (2)
N6—Fe1—N1	141.68 (7)	N4—C8—C11	107.9 (2)
N6—Fe1—N2	86.29 (7)	C9—C8—N4	109.4 (2)
N6—Fe1—N5	74.84 (7)	C9—C8—C10	111.6 (3)
N9—Fe1—N1	95.38 (8)	C9—C8—C11	111.7 (3)
N9—Fe1—N2	164.79 (8)	C11—C8—C10	109.5 (3)
N9—Fe1—N5	84.21 (8)	C8—C9—H9A	109.5
N9—Fe1—N6	108.70 (8)	C8—C9—H9B	109.5
N10—Fe1—N1	108.35 (8)	C8—C9—H9C	109.5
N10—Fe1—N2	82.59 (8)	H9A—C9—H9B	109.5
N10—Fe1—N5	172.39 (8)	H9A—C9—H9C	109.5
N10—Fe1—N6	100.36 (8)	H9B—C9—H9C	109.5
N10—Fe1—N9	91.91 (8)	C8—C10—H10A	109.5
C4—N1—Fe1	122.55 (15)	C8—C10—H10B	109.5
C5—N1—Fe1	118.20 (16)	C8—C10—H10C	109.5
C5—N1—C4	118.5 (2)	H10A—C10—H10B	109.5
N3—N2—Fe1	135.06 (16)	H10A—C10—H10C	109.5
N3—N2—C6	110.07 (19)	H10B—C10—H10C	109.5
C6—N2—Fe1	110.64 (15)	C8—C11—H11A	109.5
N2—N3—N4	106.56 (18)	C8—C11—H11B	109.5
N3—N4—C8	120.84 (19)	C8—C11—H11C	109.5
C7—N4—N3	110.97 (19)	H11A—C11—H11B	109.5
C7—N4—C8	128.1 (2)	H11A—C11—H11C	109.5
C12—N5—Fe1	124.97 (15)	H11B—C11—H11C	109.5
C13—N5—Fe1	115.10 (16)	N5—C12—C3	115.17 (19)
C13—N5—C12	119.2 (2)	N5—C12—H12A	108.5
N7—N6—Fe1	135.88 (15)	N5—C12—H12B	108.5
N7—N6—C14	109.98 (18)	C3—C12—H12A	108.5
C14—N6—Fe1	113.70 (15)	C3—C12—H12B	108.5
N6—N7—N8	106.35 (18)	H12A—C12—H12B	107.5
N7—N8—C16	119.69 (19)	N5—C13—H13	121.3
C15—N8—N7	111.10 (19)	N5—C13—C14	117.4 (2)
C15—N8—C16	129.1 (2)	C14—C13—H13	121.3
C20—N9—Fe1	158.0 (2)	N6—C14—C13	118.2 (2)
C21—N10—Fe1	175.3 (2)	N6—C14—C15	107.5 (2)

H1A—C1—H1B	109.5	C15—C14—C13	134.2 (2)
H1A—C1—H1C	109.5	N8—C15—C14	105.1 (2)
H1B—C1—H1C	109.5	N8—C15—H15	127.5
C3—C1—H1A	109.5	C14—C15—H15	127.5
C3—C1—H1B	109.5	N8—C16—C17	108.3 (2)
C3—C1—H1C	109.5	N8—C16—C19	107.8 (2)
H2A—C2—H2B	109.5	C17—C16—C19	110.0 (3)
H2A—C2—H2C	109.5	C18—C16—N8	107.2 (2)
H2B—C2—H2C	109.5	C18—C16—C17	110.8 (3)
C3—C2—H2A	109.5	C18—C16—C19	112.5 (3)
C3—C2—H2B	109.5	C16—C17—H17A	109.5
C3—C2—H2C	109.5	C16—C17—H17B	109.5
C1—C3—C4	106.4 (2)	C16—C17—H17C	109.5
C2—C3—C1	109.7 (2)	H17A—C17—H17B	109.5
C2—C3—C4	111.0 (2)	H17A—C17—H17C	109.5
C2—C3—C12	110.4 (2)	H17B—C17—H17C	109.5
C12—C3—C1	106.8 (2)	C16—C18—H18A	109.5
C12—C3—C4	112.4 (2)	C16—C18—H18B	109.5
N1—C4—C3	110.89 (19)	C16—C18—H18C	109.5
N1—C4—H4A	109.5	H18A—C18—H18B	109.5
N1—C4—H4B	109.5	H18A—C18—H18C	109.5
C3—C4—H4A	109.5	H18B—C18—H18C	109.5
C3—C4—H4B	109.5	C16—C19—H19A	109.5
H4A—C4—H4B	108.1	C16—C19—H19B	109.5
N1—C5—H5	121.4	C16—C19—H19C	109.5
N1—C5—C6	117.1 (2)	H19A—C19—H19B	109.5
C6—C5—H5	121.4	H19A—C19—H19C	109.5
N2—C6—C5	117.0 (2)	H19B—C19—H19C	109.5
N2—C6—C7	107.4 (2)	N9—C20—S1	179.2 (2)
C7—C6—C5	135.5 (2)	N10—C21—S2	178.1 (2)
N4—C7—C6	105.0 (2)		

Fe1—N1—C4—C3	72.0 (2)	N7—N6—C14—C15	0.0 (3)
Fe1—N1—C5—C6	−4.9 (3)	N7—N8—C15—C14	1.3 (3)
Fe1—N2—N3—N4	154.24 (17)	N7—N8—C16—C17	−159.3 (2)
Fe1—N2—C6—C5	20.5 (3)	N7—N8—C16—C18	81.1 (3)
Fe1—N2—C6—C7	−161.09 (17)	N7—N8—C16—C19	−40.3 (3)
Fe1—N5—C12—C3	−55.6 (3)	C1—C3—C4—N1	178.3 (2)
Fe1—N5—C13—C14	−1.4 (3)	C1—C3—C12—N5	174.3 (2)
Fe1—N6—N7—N8	172.44 (16)	C2—C3—C4—N1	59.1 (3)
Fe1—N6—C14—C13	9.3 (3)	C2—C3—C12—N5	−66.5 (3)
Fe1—N6—C14—C15	−173.69 (16)	C4—N1—C5—C6	165.5 (2)
N1—C5—C6—N2	−11.6 (3)	C4—C3—C12—N5	58.0 (3)
N1—C5—C6—C7	170.7 (3)	C5—N1—C4—C3	−97.9 (3)
N2—N3—N4—C7	−0.1 (3)	C5—C6—C7—N4	178.3 (3)
N2—N3—N4—C8	−177.5 (2)	C6—N2—N3—N4	0.4 (3)
N2—C6—C7—N4	0.4 (3)	C7—N4—C8—C9	171.2 (3)
N3—N2—C6—C5	−178.9 (2)	C7—N4—C8—C10	−68.0 (4)

N3—N2—C6—C7	−0.5 (3)	C7—N4—C8—C11	49.5 (4)
N3—N4—C7—C6	−0.2 (3)	C8—N4—C7—C6	177.0 (2)
N3—N4—C8—C9	−11.8 (4)	C12—N5—C13—C14	169.1 (2)
N3—N4—C8—C10	108.9 (3)	C12—C3—C4—N1	−65.1 (3)
N3—N4—C8—C11	−133.5 (3)	C13—N5—C12—C3	134.8 (2)
N5—C13—C14—N6	−5.3 (3)	C13—C14—C15—N8	175.5 (3)
N5—C13—C14—C15	178.7 (3)	C14—N6—N7—N8	0.8 (2)
N6—N7—N8—C15	−1.3 (3)	C15—N8—C16—C17	25.7 (4)
N6—N7—N8—C16	−177.2 (2)	C15—N8—C16—C18	−94.0 (3)
N6—C14—C15—N8	−0.7 (3)	C15—N8—C16—C19	144.7 (3)
N7—N6—C14—C13	−177.0 (2)	C16—N8—C15—C14	176.7 (2)

Hydrogen-bond geometry (Å, º)

D—H···*A*	*D*—H	H···*A*	*D*···*A*	*D*—H···*A*
C4—H4*B*···C21^{i}	0.97	2.84	3.786 (4)	166
C5—H5···S1^{ii}	0.93	2.99	3.718 (4)	137
C7—H7···S1^{i}	0.93	2.90	3.764 (4)	155
C13—H13···S1^{iii}	0.93	2.99	3.724 (4)	137
C13—H13···C20^{iii}	0.93	2.75	3.558 (4)	146
C15—H15···S1^{iii}	0.93	2.84	3.573 (4)	137
C17—H17*A*···S2^{iv}	0.96	2.94	3.873 (4)	166
C17—H17*B*···S2^{v}	0.96	2.94	3.850 (4)	158

Symmetry codes: (i) −*x*+1, −*y*+2, −*z*+1; (ii) *x*+1, *y*, *z*; (iii) −*x*, −*y*+1, −*z*+1; (iv) *x*, *y*−1, *z*; (v) −*x*, −*y*+1, −*z*.